

Angle-resolved photoemission investigation of the electronic structure of Be: Surface states

R. A. Bartynski, E. Jensen, T. Gustafsson, and E. W. Plummer
*Department of Physics and Laboratory for Research on the Structure of Matter,
 University of Pennsylvania, Philadelphia, Pennsylvania 19104*

(Received 15 February 1985)

We have performed an angle-resolved photoemission investigation, using synchrotron radiation, of the surface electronic structure of Be(0001). At normal emission we observe a surface state in the $\Gamma_3^+-\Gamma_4^-$ band gap with a binding energy of 2.8 ± 0.1 eV. Away from $\bar{\Gamma}$ it disperses parabolically towards E_F with an effective mass of $m^*/m \sim 1.5$. For $\hbar\omega < 40$ eV, the energy dependence of the photoexcitation cross section for this state shows rapid variations caused by changes in the local electromagnetic field at the surface. For $\hbar\omega > 40$ eV, it shows only weak structure. This high-energy behavior is quite different from the large resonances observed for surface states on other metals and is associated with the short penetration depth of the Be surface state. The dispersion of this state is measured along $\bar{\Gamma} \rightarrow \bar{M}$ and $\bar{\Gamma} \rightarrow \bar{K}$ in the two-dimensional surface Brillouin zone. For a small range of k_{\parallel} around \bar{M} , there is evidence for *two surface states* in the $M_2^- - M_4^-$ gap with binding energies of 1.8 ± 0.1 eV and 3.0 ± 0.1 eV.

I. INTRODUCTION

Surface states have been predicted theoretically and observed by photoemission on many metal surfaces.¹⁻⁷ Defined as two-dimensional Bloch states localized on the surface, they may disperse with momentum parallel to the surface (k_{\parallel}) but not with perpendicular momentum (k_{\perp}). True surface states exist in regions of energy and momentum space forbidden to bulk states (i.e., band gaps), while surface resonances may overlap the bulk states.

With angle-resolved photoelectron spectroscopy, the binding energy of a surface state can be measured as a function of angle and its dispersion with k_{\parallel} determined. The surface-state peak may show intensity variations with photon energy which can be related to the nature of the surface-state wave function.^{2,4,7}

We have performed angle-resolved photoemission measurements on the Be(0001) surface in an effort to determine directly its electronic structure. Both surface and bulk features are observed in the spectra. As our results for the bulk states are discussed elsewhere,^{8,9} the present paper is restricted to the surface states. Data were collected at normal emission in the photon energy range of 10–110 eV. Off-normal emission spectra, taken at several different photon energies, were confined to the $\bar{\Gamma} \rightarrow \bar{M}$ and $\bar{\Gamma} \rightarrow \bar{K}$ symmetry lines of the surface Brillouin zone (SBZ) and covered over 1.5 zones in k_{\parallel} . Polarization selection rules were employed to determine the symmetry of the surface state with respect to the mirror plane of the crystal surface. As first reported by Karlsson *et al.*⁵ a surface state with a binding energy of 2.8 eV at $\bar{\Gamma}$ exists in the $\Gamma_3^+-\Gamma_4^-$ bulk band gap and is of even symmetry with respect to the mirror operation of the hexagonal surface. The variation of intensity with photon energy of this surface state at normal emission shows no pronounced dependence on the final-state band structure of the solid. This is different from what has been reported for similar states on several other metal surfaces.^{2,4,6,7} The surface

state disperses towards the Fermi energy (E_F) as k_{\parallel} increases and the bulk band gap closes. At larger k_{\parallel} , another gap opens up near \bar{M} and a surface state, which disperses symmetrically about \bar{M} , appears. We also observe an intense peak which appears for only a narrow range of k_{\parallel} , near the \bar{M} point. This peak shows no dispersion over a wide range of photon energies and is probably a *second* surface state existing in the $M_2^- - M_4^-$ bulk band gap.

The remainder of this paper is organized as follows. Section II describes the experimental apparatus and procedures, along with some details about the hcp (0001) surface. In Sec. III we present our results on the photoexcitation cross section at normal emission and on the dispersion with k_{\parallel} , with special emphasis on the \bar{M} region where the second surface state occurs. Section IV discusses the origin of these features, while Sec. V summarizes our results and conclusions.

II. EXPERIMENTAL PROCEDURE

The data were taken at the Synchrotron Radiation Center of the University of Wisconsin in Stoughton, Wisconsin. The light, in the energy range 10–110 eV, was dispersed by a toroidal grating monochromator.¹⁰ The electrons were analyzed with a hemispherical electrostatic analyzer having an acceptance angle of $\pm 2.5^\circ$.¹¹ The experimental chamber is a standard μ -metal-shielded stainless-steel ultra-high-vacuum chamber with a base pressure of 1×10^{-10} Torr. The chamber was equipped with low-energy electron diffraction (LEED) optics for surface structural determination and a cylindrical mirror analyzer for Auger electron spectroscopy (AES) and angle-integrated photoemission measurements.

Our procedure for sample cleaning has been described elsewhere.⁹ Briefly, we argon-sputtered the crystal for several hours at room temperature to remove the initial oxide layer. To remove a small residual oxygen layer,

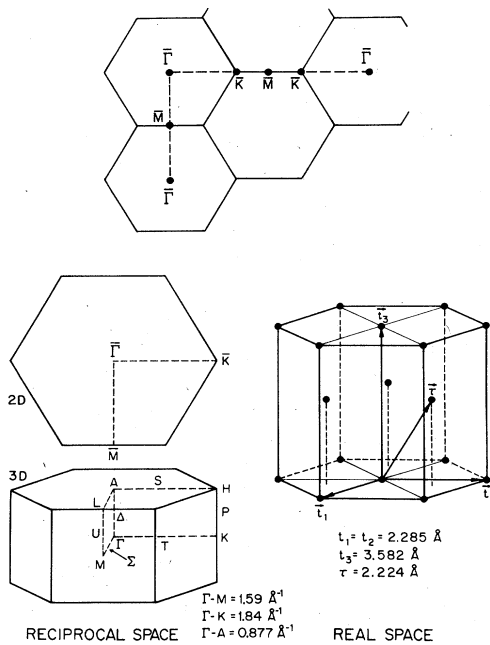


FIG. 1. Real- and reciprocal-space lattices of Be(0001). The top of the figure shows the extended surface Brillouin zone. Note that the length of the vector τ was given incorrectly in Ref. 9. 2D indicates the two-dimensional surface Brillouin zone, 3D the three-dimensional bulk Brillouin zone.

sputtering at $\sim 450^\circ\text{C}$ was necessary. This procedure gave a fair quality, sixfold LEED pattern and no trace of contamination in AES.

Figure 1 shows the real- and reciprocal-space unit cells for the Be hcp structure. The symmetry notation of Herring is used.¹² For the (0001) surface the Γ -to- A direction is the crystal normal, i.e., $\bar{\Gamma}$ in the two-dimensional SBZ. Figure 1 shows also the extended SBZ which is explored in off-normal emission. We have restricted our attention to the $\bar{\Gamma} \rightarrow \bar{M}$ and the $\bar{\Gamma} \rightarrow \bar{K}$ symmetry lines of the SBZ. As k_{\parallel} is increased along $\bar{\Gamma} \rightarrow \bar{M}$, the center of the zone face is reached at $k_{\parallel} = 1.59 \text{ \AA}^{-1}$. Then the second zone is entered and one moves towards $\bar{\Gamma}$ (located at $k_{\parallel} = 3.18 \text{ \AA}^{-1}$) in the second SBZ. Along $\bar{\Gamma} \rightarrow \bar{K}$, however, the situation is not so simple. First $\bar{\Gamma} \rightarrow \bar{K}$ is traversed, then one moves along the zone edge, $\bar{K} \rightarrow \bar{M} \rightarrow \bar{K}$, and finally back along $\bar{K} \rightarrow \bar{\Gamma}$ reaching $\bar{\Gamma}'$ at $k_{\parallel} = 5.52 \text{ \AA}^{-1}$.

III. RESULTS

Figure 2 shows a series of photoemission spectra taken at normal emission. The broad, high binding-energy peak, which disperses with photon energy, is a bulk transition between states along the Δ axis and is discussed elsewhere.^{8,9} The sharp, intense peak seen at $2.8 \pm 0.1 \text{ eV}$ binding energy is the surface state of interest here. When compared to the calculated (measured) bulk states^{9,13} along Δ we see that it lies a full 1.5 eV (2.0 eV) above the

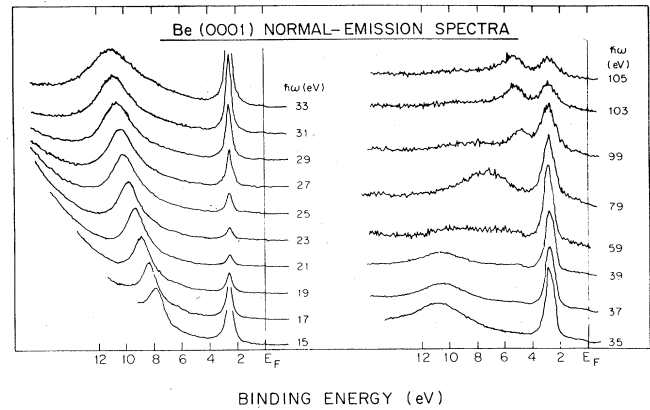


FIG. 2. Normal-emission-photoelectron spectra of Be(0001) at different photon energies. The photon angle of incidence was 45° .

band edge. The $\Gamma_3^+ - \Gamma_4^-$ gap in Be is calculated to be 6 eV wide,⁹ so the surface state is near the middle of the gap. This is in contrast to what has been observed on other simple and noble metals.^{1-4,6,7} In those systems the surface state lies just above the lower band edge. In a simple picture, the depth to which a surface state extends into the bulk is inversely related to both its distance from the band edge and the gap size.¹⁴ From this we expect the Be $\bar{\Gamma}$ surface state to be more localized on the surface than the corresponding states seen on other simple metals.

The large energy separation between the Be surface state and bulk bands also affects the surface-state line shape. Most surface states seen on other metal surfaces are so close to the band edge that their energy width overlaps the bulk bands. For example, the surface state on Al(100) is only 0.1 eV above the bulk band and it exhibits a width of $\sim 0.5 \text{ eV}$.⁴ Likewise the Al(111) surface state has a width of $\sim 1.5 \text{ eV}$ in a 0.4-eV gap.⁷ These surface states exhibit line shapes which are asymmetric and cannot be fit with either a Gaussian or a Lorentzian curve. We have analyzed the line shape of the Be normal-emission surface state in detail. After a linear background is subtracted from the data, the peak is fit by a Lorentzian, as shown in Fig. 3, with a full width at half maximum of 0.46 eV. This is one of the first examples of a truly Lorentzian line shape from a surface state. The very weak intensity seen at the Fermi energy makes it impossible to measure directly the instrumental resolution, but equivalent monochromator and analyzer settings in experiments on other materials have shown that the instrumental resolution is 0.10 to 0.15 eV. This would imply an inherent linewidth of 0.43 to 0.45 eV for the Be $\bar{\Gamma}$ state.

The spectra in Fig. 2 are scaled so that both bulk and surface features may be seen. It is interesting to note that for the entire photon energy range from about 30 to 105 eV, the surface state is the dominant feature. We show the surface-state intensity as a function of photon energy in Fig. 4. The raw data have been corrected for the photon-energy-dependent efficiency of the monochromator but not for the electron-energy-dependent transmission function of the electron analyzer. The latter quantity is

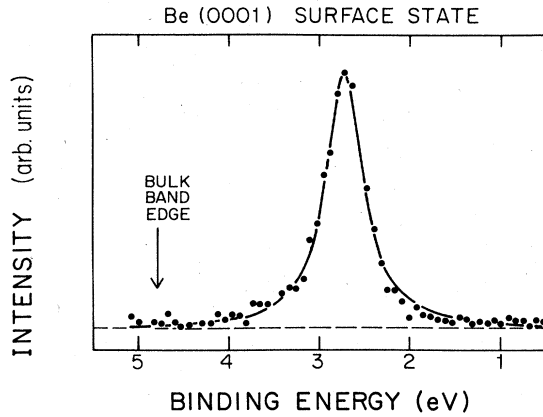


FIG. 3. Lorentzian fit to the surface state at $\bar{\Gamma}$ for $\hbar\omega = 37$ eV.

expected to vary slowly as a function of electron kinetic energy and should not introduce any spurious features into this curve. The sharpness of the surface state and the low background emission within the first few eV below E_F have allowed us to measure its intensity as it varies over four orders of magnitude while $\hbar\omega$ varies over 100 eV. For comparison the data for the Al(100) surface state are also shown.^{4,15}

There is well-defined structure in the photon-energy dependence of the intensity for low excitation energies ($\hbar\omega < 40$ eV). At higher photon energies we see only broad and weak features, one near 60 eV and another near

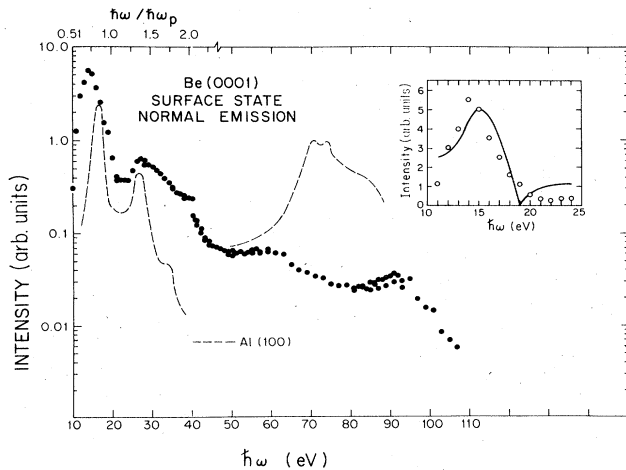


FIG. 4. Semilogarithmic plot of the surface-state intensity at $\bar{\Gamma}$ as a function of $\hbar\omega$. The angle of incidence was 45° . The dashed curve shows the intensity profile for the Al(100) surface state.⁴ The low-energy Al data are plotted as a function of $\hbar\omega/\hbar\omega_p$ (the upper horizontal axis). The high-energy Al data is plotted on the same horizontal scale as the Be data (the lower horizontal axis). The Be data may of course be referenced to either scale. The inset shows the low-energy data for Be on a linear intensity scale. The solid line is the calculation from Ref. 15, scaled to account for the difference in plasmon energy between Be and Al.

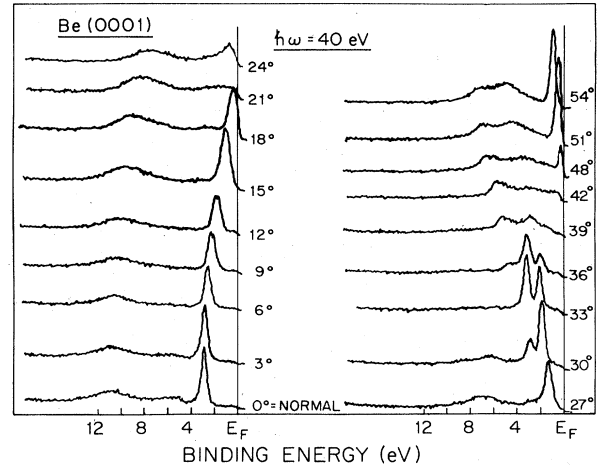


FIG. 5. Photoelectron spectra of Be(0001) at $\hbar\omega = 40$ eV for different electron emission angles θ along the $\bar{\Gamma} \rightarrow \bar{M}$ azimuth. The photon angle of incidence was 45° and electrons were collected in the plane of incidence.

90 eV. The high-energy features are superimposed on a very rapidly decreasing background which necessitates presentation of the data on a semilogarithmic scale. We will attribute the low-energy structure ($\hbar\omega < 40$ eV) to the surface photoeffect, while the high-energy behavior ($\hbar\omega > 40$ eV) will be shown to be a consequence of the short penetration depth of the surface state.

When the electron analyzer is moved away from the crystal normal, the collected electrons have finite momentum parallel to the surface as given by the expression

$$k_{\parallel} = \left[\frac{2mE_k}{\hbar^2} \right]^{1/2} \sin\theta,$$

where E_k is the kinetic energy of the detected electrons and θ is the angle between the collection direction and the crystal normal. Since neither the presence of the surface nor the dipole excitation process breaks the crystal symmetry parallel to the surface, k_{\parallel} is conserved. Thus, one may analyze electrons emitted at finite polar angles and investigate initial states away from $\bar{\Gamma}$.

Spectra taken at $\hbar\omega = 40$ eV for a series of polar angles along the $\bar{\Gamma} \rightarrow \bar{M}$ azimuth are shown in Fig. 5. The surface state is seen at 2.8 eV binding energy in the normal-emission spectrum. As θ becomes nonzero, the spectral feature disperses upward, reaching E_F at 18° (0.94 \AA^{-1}). Near 24° (1.23 \AA^{-1}) another sharp feature appears which disperses downward as θ increases, reaching a local maximum in binding energy of 1.8 ± 0.1 eV near 33° (1.65 \AA^{-1}), approximately the \bar{M} point of the SBZ. A second, sharp feature is seen in the region of k_{\parallel} near \bar{M} in the 30° , 33° , and 36° spectra. It has a higher binding energy than the state first seen near \bar{M} . For angles outside this small range it is, if detectable, very weak and broad. The state disperses slightly with k_{\parallel} reaching a maximum binding energy of 3.0 ± 0.1 eV near 33° ($\sim 1.65 \text{ \AA}^{-1}$). At $\theta = 48^\circ$ ($k_{\parallel} = 2.25 \text{ \AA}^{-1}$) the surface state first seen near normal emission reappears at E_F and disperses downward with

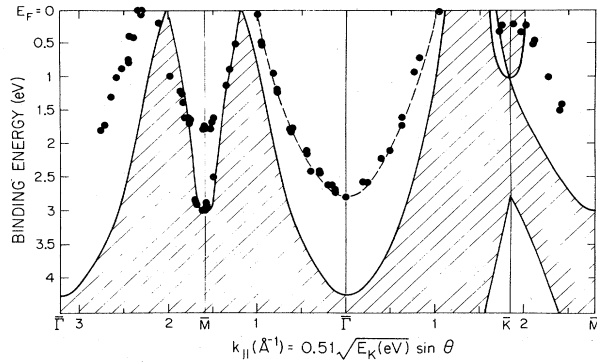


FIG. 6. Dispersion of the surface state(s) on Be(0001) as a function of parallel momentum (k_{\parallel}). The shaded region is the projection of the calculated bulk bands from Ref. 13.

increasing angle as $\bar{\Gamma}$ in the second zone is approached. The peaks seen at binding energies greater than 3 eV are attributed to bulk transitions.

The surface-state binding energy as a function of k_{\parallel} along the $\bar{\Gamma} \rightarrow \bar{M}$ and $\bar{\Gamma} \rightarrow \bar{K}$ axes is plotted in Fig. 6 with the projection of the calculated bulk bands along these symmetry directions.¹³ We see that the surface state near $\bar{\Gamma}$ remains well outside the bulk bands. For $1.2 \text{ \AA}^{-1} < k_{\parallel} < 1.4 \text{ \AA}^{-1}$ and $1.9 \text{ \AA}^{-1} < k_{\parallel} < 2.2 \text{ \AA}^{-1}$ along $\bar{\Gamma} \rightarrow \bar{M}$, the surface state near \bar{M} overlaps the calculated bulk bands. These regions correspond to the $\theta = 24^\circ$ and $\theta = 39^\circ$ spectra in Fig. 5, where the surface states have become broad and ill-defined spectral features. This is attributed to the interactions with the underlying bulk bands and the surface state should probably be viewed as a surface resonance here. For the $27^\circ < \theta < 36^\circ$ and the $\theta > 48^\circ$ spectra of Fig. 5, the states are sharp as they reside in band gaps. The transition from a true surface state to a surface resonance occurs in an angular range smaller than the angular acceptance of our analyzer preventing a detailed study of this effect.

IV. DISCUSSION

For photon energies below 40 eV, the intensity profile shown in Fig. 4 is characterized by strong emission near $\hbar\omega = 14$ eV, suppressed emission near $\hbar\omega = 23$ eV, and then enhancement again near 30 eV. These features have the same origin as the very similar intensity variation exhibited by the Al(100) surface state in the energy range $\hbar\omega < 30$ eV (Ref. 15) shown as the dashed line in Fig. 4. This behavior is due to the rapid variations of the effective vector potential at the metal surface as the photon energy passes through the threshold for plasmon production ($\hbar\omega_p = 15.3$ eV in Al and 19.5 eV in Be). The inset in Fig. 4 shows the data for Be on a linear intensity scale along with the results of a calculation for a jellium surface with the Al electron density.¹⁵ The height of the calculated curve was adjusted to fit the data best and the energy axis was rescaled by a factor of $\hbar\omega_p(\text{Be})/\hbar\omega_p(\text{Al})$ to compare the results in natural units. We find that the shape and position of the experimental profile is reproduced quite

well by this curve, but the agreement is not as good as was found for the Al surface state.¹⁵ This is probably because Al is much more free-electron-like than Be and is therefore better described by a jellium calculation. Be has strong interband transitions near the plasmon energy which broaden the plasmon excitation.⁸ Large band gaps and a low density of states at E_F further illustrate how Be deviates from free-electron-like behavior.^{8,9}

Resonances in the photoexcitation cross section of surface states have been observed above the plasmon energy on several simple metals.^{2,4,6,7} They have often been successfully described in terms of a model first put forward by Louie *et al.*² Its main features are as follows: The wave function ψ_s for a surface state of parallel momentum k_{\parallel} and binding energy E_{SS} may be written as a superposition of all bulk states of the same k_{\parallel} in the form

$$\psi_s = \sum_{n, k_{\perp}} a_n(k_{\perp}) \phi_n(k_{\perp}), \quad (1)$$

where the sum is over all perpendicular momenta k_{\perp} and bands n . The intensity of emission, within a direct-transition model, is given by the expression

$$I_s(\omega) \propto \left| \sum_n a_n(k_{\perp}) M_b^n \right|^2, \quad (2)$$

where M_b^n is a bulk matrix element for transition to a state at final energy $E_f(k_{\perp})$. Energy conservation requires $E_f(k_{\perp}) = E_{SS} + \hbar\omega$, which defines the value of k_{\perp} .

Two conditions can make the application of Eq. (2) straightforward. If the matrix elements M_b^n are constant, or only smoothly varying, their effect on the intensity profile should be small. Then the profile will be dominated by the expansion coefficients $a_n(k_{\perp})$. In addition, when the surface state is very close in energy to the bulk band edge, the function $a_n(k_{\perp})$ is strongly peaked at the k_{\perp} value of the band edge. This leads directly to sharp resonances in $I_s(\omega)$. Most previously studied surface states have satisfied these conditions and their emission intensity profiles have been successfully interpreted as resonances in $a_n(k_{\perp})$. For example, the high-energy data for Al(100) shown in Fig. 4 (dashed line) exhibit dramatic increases in intensity near 71 and 74 eV. This is where the surface state is excited into the X'_4 and X_1 points of the final bands. In beryllium, however, the surface state is found near midgap, suggesting that $a_n(k_{\perp})$ is not strongly peaked. We believe that this explains the lack of prominent resonances above 40 eV in Fig. 4. In addition, photoemission results in this energy range from the bulk⁹ indicate that the matrix elements are not slowly varying. The weak peaks observed near 60 and 90 eV may be associated with structure in $M_b^n(\omega)$; calculations predict local maxima in the bulk cross section for these final-state energies.⁹

We now turn our attention to the behavior of the surface state away from $k_{\parallel} = 0$. The dispersion of the surface state about $\bar{\Gamma}$ is quite parabolic along both $\bar{\Gamma} \rightarrow \bar{M}$ and $\bar{\Gamma} \rightarrow \bar{K}$, but the curvature is different for the two directions. Figure 6 shows the data along with free-electron-like dispersions (dashed lines). Excellent agreement is obtained along $\bar{\Gamma} \rightarrow \bar{M}$ with a free-electron band of

effective mass $m^*/m=1.53$ while $m^*/m=1.45$ fits the $\bar{\Gamma}\rightarrow\bar{K}$ data. This difference in effective mass is correlated with the different curvature of the calculated¹³ bulk band edge in the two directions. The band edges are fitted with effective masses of $m^*/m=1.16$ and 1.12 along $\bar{\Gamma}\rightarrow\bar{M}$ and $\bar{\Gamma}\rightarrow\bar{K}$, respectively.

The $\bar{\Gamma}\rightarrow\bar{M}$ line in the SBZ lies in the only mirror plane of the bulk which contains the surface normal, and we restrict further analysis to this direction. The surface electronic structure near \bar{M} is more complicated than that seen at $\bar{\Gamma}$. As mentioned above, Fig. 5 shows two sharp features in the spectra near \bar{M} , best seen in the $\theta=33^\circ$ spectrum. Figure 6 shows that the 1.8-eV peak is clearly in the band gap and can be identified as a surface state. The deeper peak appears to be located on the edge of the projected calculated bulk bands. However, results from bulk measurement of Be (Ref. 9) and other simple metals^{4,6} indicate that the measured band gaps can be larger than the calculated ones, which means that the 3-eV state may indeed lie outside the bulk bands. Figure 7 shows several spectra taken at \bar{M} over a wide range of photon energies. The two peaks at 1.8 and 3.0 eV do not show any dispersion, while a deeper bulk peak [seen in the (42–54)-eV spectra] moves as the photon energy is varied. The similarity of the line shapes of the two nondispersing peaks is striking, particularly when compared to that of

the bulk state. If we perform the same linewidth analysis on the two surface states at \bar{M} as was done earlier on the $\bar{\Gamma}$ surface state (Fig. 3), we find an inherent width of 0.38 eV (0.50 eV) for the 1.8-eV (3-eV) states. This narrow width compared to any width observed for a bulk transition⁹ is very strong evidence that both peaks are surface states. In addition, Figs. 5 and 6 show that both states become ill-defined when they overlap the projected bulk bands.

Several authors have previously tried to determine the number of surface states that can exist in a given band gap. A nearly-free-electron (NFE) —like model used by Forstmann¹⁶ predicts one surface state in such gaps. Pendry and Gurman¹⁷ conclude, based on a more general but physically less transparent scattering calculation, that a gap at the center of the Brillouin zone or on the zone face can support zero or one state, whereas an internal gap can support one or two. In these studies, the potential at the interface was terminated abruptly. Garcia and Solana¹⁸ showed that, even on a zone face, more than one surface state may exist in a gap if an image-type surface potential is assumed. However, the states in Fig. 7 are far below the vacuum level and we believe that it is very unlikely that the image potential affects them.

Bartynski *et al.*,¹⁹ in a study of Cu(110), have obtained results similar to Pendry and Gurman by using a NFE approach. The departure from the earlier results by Forstmann is due to differences in the location of the plane where the internal and external wave functions are matched. The situation on Be(0001) is qualitatively similar to that on Cu(110). The bulk bands along $M-L$ are shown in Fig. 8. There is a double degeneracy at L (left panel), which is due to the fact that we have chosen to use the conventional real-space unit cell (Fig. 1) and not the primitive unit cell. When the bands are unfolded around L and plotted for positive and negative k_\perp , two gaps separated by less than a reciprocal-lattice vector are observed (right panel). It is then possible to have either one or two surface states.¹⁹ the number of surface states that actually occurs depends on the parameters which characterize each particular case.

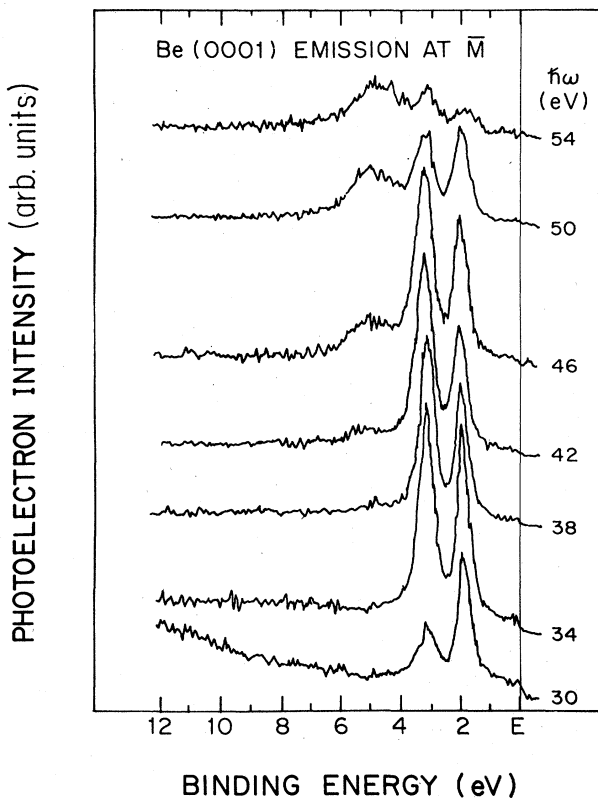


FIG. 7. Photoelectron spectra for the region around \bar{M} in the surface Brillouin zone. The collection angle has been changed with photon energy so that the 3-eV peak originates from \bar{M} . The angle of photon incidence was 45° from the normal and electrons were collected in the plane of incidence.

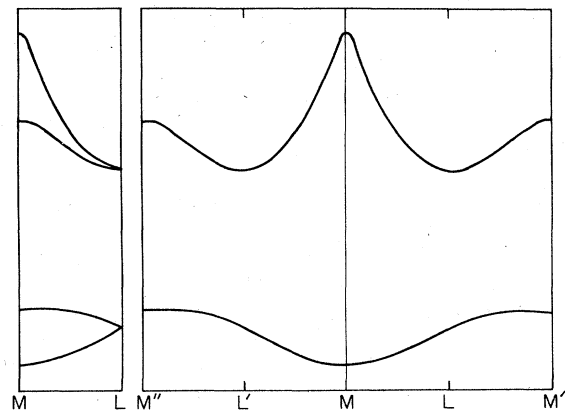


FIG. 8. Bulk band structure of Be(0001) along the $L-M$ (\bar{M}) direction in reciprocal space.⁹

The electronic structure of Be is qualitatively similar to that of Mg. They both have hcp crystal structure and have two conduction electrons per atom. Two major quantitative differences are that the Mg band gaps are much smaller than those in Be, and that in Mg there are *occupied* states on both sides of the gaps at $\bar{\Gamma}$. Angle-resolved photoemission data on Mg(0001) (Refs. 3 and 6) show a surface state at $\bar{\Gamma}$ with a dispersion similar to that on Be. The Mg state also reappears in the gap around \bar{M} but there is no evidence for a second state.^{3,6} We are not aware of any experimental evidence for *two* occupied surface states in the same gap on any other metal surface.

V. CONCLUSIONS

We have confirmed the existence of a surface state at $\bar{\Gamma}$ on Be(0001) (Ref. 5) and discussed its dispersion and cross section in detail. The dispersion with k_{\parallel} of this surface state is well described by a free-electron behavior with an effective mass of approximately $1.5m_e$. Similar *s-p* band gaps in the projected bulk band structure in the center of the Brillouin zone of the hexagonal surfaces of Al, Mg, and the noble metals also support surface states. However, the large energy separation of the Be surface state from the neighboring bulk bands results in both qualitative and

quantitative differences in the behavior of this state. For low photon energies, dramatic structure in the cross section is related to the surface photoeffect, very reminiscent of the Al(100) surface state.¹⁵ At high energies, in contrast to Cu(111) (Ref. 2), Al(100) (Ref. 4), Mg(0001) (Ref. 6), and Al(111) (Ref. 7), no pronounced resonances are observed.

In a second band gap, which occurs around the \bar{M} point of the SBZ, we find another surface state with a binding energy of 1.8 eV at \bar{M} . In a small range of k_{\parallel} around \bar{M} , we find a second surface state in that same band gap.

ACKNOWLEDGMENTS

We thank D. Fowler, J. Blakely, and B. Addis of the Cornell Materials Science Center for supplying the sample, the Tantalus Electron Storage Ring staff for their assistance, M. Y. Chou and M. L. Cohen for supplying extensive details of their bulk-band calculations, and Paul Soven for numerous helpful discussions. This research was supported by the National Science Foundation Materials Research Laboratory program under Grant No. DMR-82-16718. The storage ring is supported by NSF Grant No. DMR-80-20164.

¹The first surface state in a free-electron-like band gap was observed by P. O. Gartland and B. J. Slagsvold, Phys. Rev. B **12**, 4047 (1975). Some additional investigations of particular importance to the present work are Ref. 2–7 below.

²S. G. Louie, P. Thiry, R. Pinchaux, Y. Petroff, D. Chanderis, and J. Lecante, Phys. Rev. Lett. **44**, 549 (1980).

³U. O. Karlsson, G. Hansson, P. Persson, and S. A. Flodstrom, Phys. Rev. B **26**, 1852 (1982).

⁴H. J. Levinson, F. Greuter, and E. W. Plummer, Phys. Rev. B **27**, 727 (1983).

⁵U. O. Karlsson, S. A. Flodstrom, R. Engelhardt, W. Gadeke, and E. E. Koch, Solid State Commun. **49**, 711 (1984).

⁶R. A. Bartynski, R. H. Gaylord, T. Gustafsson, and E. W. Plummer (unpublished). Normal emission angle-resolved photoemission results from Mg(0001) in the 10 eV $< \hbar\omega < 100$ eV range show that the surface state in the $\Gamma_3^+ - \Gamma_4^-$ gap, first reported in Ref. 3, has a binding energy of 1.6 eV, about 0.1 eV above the lower band edge. In addition, the state shows a dramatic intensity resonance near 44 eV, corresponding to transitions into the Γ_4^- point of the unoccupied bands.

⁷S. D. Kevan, N. G. Stoffel, and N. V. Smith, Phys. Rev. B **31**, 1788 (1985).

⁸E. Jensen, R. A. Bartynski, T. Gustafsson, and E. W. Plum-

mer, Phys. Rev. Lett. **52**, 2172 (1984).

⁹E. Jensen, R. A. Bartynski, T. Gustafsson, E. W. Plummer, M. Y. Chou, M. L. Cohen, and G. B. Hoflund, Phys. Rev. B **30**, 5500 (1984).

¹⁰B. P. Tonner, Nucl. Instrum. Methods **172**, 133 (1980).

¹¹C. L. Allyn, T. Gustafsson, and E. W. Plummer, Rev. Sci. Instrum. **49**, 1197 (1978).

¹²C. Herring, J. Franklin Inst. **233**, 525 (1942).

¹³P. O. Nilsson, G. Arbman, and T. Gustafsson, J. Phys. F **4**, 1937 (1974).

¹⁴E. T. Goodwin, Proc. Cambridge Philos. Soc. **35**, 221 (1939).

¹⁵H. J. Levinson, E. W. Plummer, and P. J. Feibelman, Phys. Rev. Lett. **43**, 952 (1979); H. J. Levinson and E. W. Plummer, Phys. Rev. B **24**, 628 (1981); H. J. Levinson, Ph.D. thesis, University of Pennsylvania, 1980 (unpublished).

¹⁶F. Forstmann, Z. Phys. **235**, 69 (1970).

¹⁷S. J. Gurman and J. B. Pendry, Phys. Rev. Lett. **31**, 637 (1973); J. B. Pendry and S. J. Gurman, Surf. Sci. **49**, 87 (1975).

¹⁸N. Garcia and J. Solana, Surf. Sci. **36**, 262 (1973).

¹⁹R. A. Bartynski, T. Gustafsson, and Paul Soven, Phys. Rev. B **31**, 4745 (1985).